Enzymatic Reaction of Hydrogen Peroxide-Dependent Peroxygenase Cytochrome P450s: Kinetic Deuterium Isotope Effects and Analyses by Resonance Raman Spectroscopy

Isamu Matsunaga,*,‡ Akari Yamada,§ Dong-Sun Lee,§ Eiji Obayashi,§ Nagatoshi Fujiwara,|| Kazuo Kobayashi,|| Hisashi Ogura,‡ and Yoshitsugu Shiro§

Department of Virology and Department of Host Defense, Osaka City University, Graduate School of Medicine, 1-4-3 Asahi-machi, Abeno-ku, Osaka 545-8585, Japan, and RIKEN Harima Institute/SPring-8, 1-1-1 Kouto, Mikazuki-cho, Sayo, Hyogo 679-5148, Japan

Received October 3, 2001; Revised Manuscript Received November 19, 2001

ABSTRACT: Cytochromes $P450_{SP\alpha}$ (CYP152B1) and $P450_{BS\beta}$ (CYP152A1), which are isolated from *Sphingomonas paucimobilis* and *Bacillus subtilis*, respectively, belong to the P450 superfamily, but catalyze hydroxylation reactions, in which an oxygen atom from H_2O_2 is efficiently introduced into fatty acids (e.g., myristic acid). $P450_{SP\alpha}$ produces the α-hydroxylated (α-OH) products at 100%, while $P450_{BS\beta}$ produces α- and β-hydroxylated (β-OH) products at 33 and 67%, respectively. Using deuterium-substituted fatty acids ([2,2-d_2]-myristic acid and d_{27}-myristic acid) as a substrate, the peroxygenase reactions of the two bacterial P450s were investigated. In the $P450_{SP\alpha}$ reaction, we observed an intermolecular noncompetitive kinetic isotope effect on V_{max} ($^{D}V = 4.1$) when [2,2-d_2]-myristic acid was used, suggesting that an isotopically sensitive step involving the α-hydrogen of the fatty acid is present in the catalytic cycle. On the other hand, $^{D}(V/K)$ was masked, in sharp contrast to the features of usual monooxygenases P450. The characteristic kinetic features can be interpreted in terms of the faster product formation than the substrate dissociation. A similar kinetic isotope effect was observed [$^{D}V = 4.9$, $^{D}(V/K) \sim 1$] for the $P450_{BS\beta}$ reaction, when d_{27}-myristic acid was used as a substrate, indicating that the reaction mechanism is the same for both peroxygenases. The resonance Raman spectral data of $P450_{BS\beta}$ in the ferric and ferrous−CO forms in the presence and absence of myristic acid demonstrated that the catalytic pocket of the enzyme is polar, so that the location of the carboxylate of the substrate close to the sixth ligand of the heme could be allowed. On the basis of these results on the kinetic isotope effects and spectroscopy, we discuss the possible mechanisms of the α- and β-hydroxylation of fatty acids catalyzed by peroxygenases $P450_{SP\alpha}$ and $P450_{BS\beta}$.

We have studied two unusual bacterial cytochrome P450 (P450)[1] enzymes, both of which hydroxylate a carbon adjacent to the carboxyl carbon of fatty acids. $P450_{SP\alpha}$ [systematic nomenclature (*1*), CYP152B1], identified in *Sphingomonas paucimobilis*, specifically hydroxylates an α-carbon of fatty acid substrates (*2*), and $P450_{BS\beta}$ [systematic nomenclature (*1*), CYP152A1] from *Bacillus subtilis* can attack the β-position as well as the α-position of a fatty acid to produce both β- and α-hydroxyl products (*3*). Both the enzymes efficiently introduce an oxygen atom derived from H_2O_2 to the substrate, and catalytic turnovers of these enzymes are very high (*3*−*5*), although their K_m values for H_2O_2 are very low (10^{-2} mM magnitude). These high activities are specific for H_2O_2, but alkyl hydroperoxides often used for mechanistic study on P450-containing reactions are not effective. Moreover, our previous work showed that the NADH-supported α-hydroxylation activity of fatty acids in the crude extract from *S. paucimobilis* was completely inhibited by catalase (*6*, *7*) and NADH, ferredoxin, ferredoxin reductase, and the peroxygenase P450 did not reconstitute the activities of these P450 enzymes (unpublished results). Therefore, it is unlikely that these P450s require a reduction system of molecular oxygen for their catalysis. Based on these findings, we considered that these bacterial P450 enzymes specifically require H_2O_2 for their catalytic activities and, therefore, should be appropriately designated as *peroxygenase* rather than *monooxygenase*. Compared with the usual monooxygenase P450s, there are two characteristic properties in the enzymatic reactions of peroxygenases $P450_{SP\alpha}$ and $P450_{BS\beta}$: utilization of H_2O_2 in place of O_2, and the site specificity of the reaction.

It is generally accepted that the monooxygenase P450 reaction (*8*) proceeds as follows: the substrate binds to ferric P450 (step 1); the ferric P450−substrate complex receives

* Correspondence should be addressed to this author at the Department of Virology, Osaka City University, Graduate School of Medicine, 1-4-3 Asahi-machi, Abeno-ku, Osaka 545-8585, Japan. E-mail address: matsunagai@med.osaka-cu.ac.jp. Tel: +81-6-6645-3911. FAX: +81-6-6645-3912.

‡ Department of Virology, Osaka City University.

§ RIKEN Harima Institute/SPring-8.

|| Department of Host Defense, Osaka City University.

[1] Abbreviations: GC-MS, gas chromatography−mass spectrometry; P450, cytochrome P450; $P450_{SP\alpha}$, fatty acid α-hydroxylating P450 from *Sphingomonas paucimobilis*; $P450_{BS\beta}$, fatty acid β- or α-hydroxylating P450 from *Bacillus subtilis*.

10.1021/bi011883p CCC: $22.00
Published on Web 01/17/2002

one electron from NAD(P)H to yield a ferrous P450−substrate complex (step 2); this complex combines with molecular oxygen to produce an oxygenated form (step 3); a second electron from NAD(P)H and a proton to the oxygenated form yields a hydroperoxy complex (step 4); a second protonation leads to heterolytic cleavage of the O−O bond, resulting in a highly reactive intermediate (step 5); insertion of the activated oxygen into the substrate is believed to occur by way of C−H bond cleavage, followed by rapid oxygen rebound to form a product (step 6). Newcomb et al. (*9*), however, proposed another mechanism, instead of steps 5 and 6, in which OH^+ is inserted from the iron−hydroperoxy complex to the substrate.

In the monooxygenase P450-containing system, hydrogen peroxide and alkyl hydroperoxides such as cumene hydroperoxide are sometimes used as surrogates for the reduction system and molecular oxygen (peroxide shunt pathway) to skip steps 2−4. However, the turnover rate in the hydroperoxide-supported system is generally much lower than that in the reduction system-supported catalytic cycle. In contrast, in the peroxygenase P450 ($P450_{SP\alpha}$ and $P450_{BS\beta}$) reaction, the shunt pathway is the main route to provide hydroxylated products of fatty acids, and the turnover numbers are extremely high (1000 min^{-1}).

On the site specificity of the reaction, the α- and *β*-hydroxylations of fatty acids by $P450_{SP\alpha}$ and $P450_{BS\beta}$ are very unique, compared to monooxygenase P450s, which have been known to catalyze the hydroxylation at the *ω-n* (n = 1, 2, 3) site of fatty acids. Structural differences in the substrate recognition must be responsible for the difference in the site specificity of the reaction between peroxygenases $P450_{SP\alpha}$ and $P450_{BS\beta}$ and the usual monooxygenase P450s.

The two characteristic properties in the reaction of $P450_{SP\alpha}$ and $P450_{BS\beta}$ are highly attributable to the uniqueness of their protein structure at the active site, which are possibly related to the uniqueness of the reaction mechanism. To address these issues, we investigated the effect of deuterium substitution on fatty acid hydroxylation by the peroxygenase P450s and the structural characterization of the heme environment with resonance Raman spectroscopy. A kinetic hydrogen isotope effect has been examined for many P450 reactions (*10*−*13*), and has provided useful information in restricting candidate mechanisms to those involving a C−H bond cleavage step. On the other hand, resonance Raman spectroscopy is a powerful tool to characterize the heme environmental (active site) structures of hemoproteins including P450s, by monitoring appropriate bands such as *ν*3, *ν*4, and *ν*Fe−CO. On the basis of these results obtained in this study, we could discuss the possible reaction mechanisms of fatty acid hydroxylation by peroxygenase P450s. Since the peroxygenase enzymes might be useful for industrial applications because of their unique property of being functional even in the absence of a reduction system such as NADPH−P450 reductase, it is important to clarify the reaction mechanisms responsible for their modulating functions. This knowledge may aid the development of enzymes with novel functionality using future protein engineering methods.

MATERIALS AND METHODS

Materials. Myristic acid and α-hydroxylauric acid were purchased from Sigma-Aldrich Japan (Tokyo, Japan). [2,2-d_2]-Myristic acid, d_{27}-myristic acid, and 9-anthryldiazomethane were purchased from Funakoshi Co. Ltd. (Tokyo, Japan). Other reagents were purchased from Wako Pure Chemical Industries, Ltd. (Osaka, Japan).

Preparation of Recombinant Forms of Peroxygenase P450s and Assay for Hydroxylation Activities of Myristic Acid. Expression in *Escherichia coli* and purification of recombinant forms of $P450_{SP\alpha}$ (*14*) and $P450_{BS\beta}$ (*15*) were described previously. Assay methods for the myristic acid hydroxylating activities of $P450_{SP\alpha}$ (*2*) and $P450_{BS\beta}$ (*15*) were presented elsewhere. In the current work, the reaction time was 2 min, and α-hydroxylauric acid was used as an internal standard in each enzyme assay. The deuterated substrates were stored in d_6-ethanol until use. On commencing an experiment, the substrates were diluted with ethanol to each desired concentration, and 1 μL of the ethanol solution was added to 0.2 mL of the reaction mixtures. Gas chromatography−mass spectrometry (GC-MS) confirmed that no substrate deuterium exchange to the solvent occurred during the experiments described above. Derivatization of the [2,2-d_2]-myristic acid metabolite by $P450_{SP\alpha}$ with diazomethane and analysis of this product with GC-MS were performed as previously described (*6*).

Spectral Analyses. The dissociation constants of $P450_{BS\beta}$ for nondeuterated myristic acid and d_{27}-myristic acid were measured spectrophotometrically at room temperature via substrate difference spectra using a Hitachi spectrophotometer U2001 (Hitachi Co. Ltd., Tokyo, Japan).

Measurement of resonance Raman spectra was performed with a JASCO NR-1800 spectrometer (Japan) modified in a single dispersion mode equipped with a liquid-nitrogen-cooled CCD detector (Princeton Instruments). The slit width for the spectral measurements was 4 cm^{-1}. The excitation wavelengths used for the measurements of the ferric enzymes and the ferrous−CO complexes were 413 nm from a Krypton ion laser (Coherent, Innova 90) and 441 nm from a He−Cd vapor laser (KIMMOM, Elect. Co. Ltd., Japan), respectively. The power of the Kr^+ and He−Cd lasers at the sample was about 50 and 10 mW, respectively. Holographic filters (KAISER OPTICAL SYSTEMS, Inc.) were used to remove the Rayleigh scattering. The cylindrical Raman cell containing the sample solution, whose concentration was 50 μM, was spun to minimize local heating and photodissociation of the iron-bound CO. The Raman spectrometer was calibrated for each measurement with indene as standard.

RESULTS

Deuterium Effect on Enzymatic Reactions Catalyzed by $P450_{SP\alpha}$. Peroxygenase $P450_{SP\alpha}$ catalyzes the reaction of a long-chain fatty acid (substrate) with H_2O_2 to specifically produce an enantiomerically pure α-[*S*]-hydroxyl product (*2*). We analyzed the reaction products using the GC-MS technique, when a deuterated fatty acid, [2,2-d_2]-myristic acid, was used as a substrate. In Figure 1, the mass chromatogram for the metabolite of this reaction is illustrated. The M^+ ion and two fragment ions produced by C1−C2 and C2−C3 cleavage, respectively, are larger by +1 than the corresponding ones of the reaction product (α-hydroxymyristic acid) from the nondeuterated substrate (*6*). The result clearly indicated that the metabolite of this reaction was α-hydroxy-[2-*d*]-myristic acid. The α-hydrogen (α-H) of the

Table 1: Kinetic Noncompetitive Isotope Effects of the Reactions of $P450_{SP\alpha}$ and $P450_{BS\beta}$

	$P450_{SP\alpha}$				$P450_{BS\beta}$			
substrates	K_m[a]	V_{max}[b]	^DV	$^D(V/K)$	K_m[a]	V_{max}[b]	^DV	$^D(V/K)$
myristic acid	41 ± 7.2	2700 ± 200			58 ± 15	320 ± 29		
[2,2-d_2]-myristic acid	14 ± 2.1	660 ± 29	4.1	1.4	58 ± 7.0	312 ± 16	1.0	1.0
d_{27}-myristic acid	nd[c]	nd[c]			17 ± 2.0	65 ± 2.3	4.9	1.4

[a] Results are shown as mean (μM) ± standard error ($n = 6$). [b] Results are shown as mean [nmol min^{-1} (nmol of P450)$^{-1}$] ± standard error ($n = 6$). [c] Not determined.

Table 2: Kinetic Isotope Effect on the Formation of α- or β-Hydroxyl Products by $P450_{BS\beta}$

	formation of α-hydroxyl product				formation of β-hydroxyl product			
substrates	K_m[a]	V_{max}[b]	^DV	$^D(V/K)$	K_m[a]	V_{max}[b]	^DV	$^D(V/K)$
myristic acid	85 ± 12	128 ± 7.8			50 ± 22	201 ± 29		
[2,2-d_2]-myristic acid	51 ± 18	21 ± 3.3	6.1	3.7	59 ± 22	290 ± 48	0.7	0.8
d_{27}-myristic acid	18 ± 0.9	19 ± 3.0	6.7	1.4	11 ± 1.4	39 ± 1.3	5.2	1.1

[a] Results are shown as mean (μM) ± standard error ($n = 6$). [b] Results are shown as mean [nmol min^{-1} (nmol of P450)$^{-1}$] ± standard error ($n = 6$).

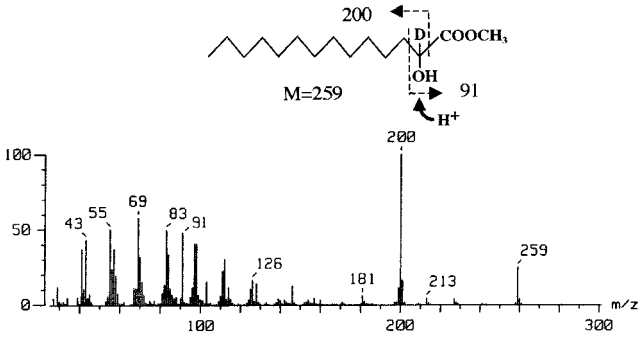

FIGURE 1: Mass spectrum of a [2,2-d_2]-myristic acid metabolite by the reaction of $P450_{SP\alpha}$. The metabolite was methylated by diazomethane for analysis.

myristic acid was abstracted and replaced with a hydoxyl group in a step of the catalytic cycle of peroxygenase $P450_{SP\alpha}$.

We investigated the effects of the deuterium substitution at the α-position of the fatty acid on the enzymatic reaction of $P450_{SP\alpha}$. In Table 1, kinetic parameters, V_{max} and K_m, of the Michaelis−Menten mechanism are presented for the two reactions, in which nondeuterated or [2,2-d_2]-myristic acid was used as a substrate. The table shows that both kinetic parameters, V_{max} and K_m, were dramatically affected by the deuterium substitution for the α-H. This result suggests that the catalytic cycle of $P450_{SP\alpha}$ contains an isotopically sensitive step, the reaction rate of which becomes significantly slow relative to those of other steps in the catalytic cycle of $P450_{SP\alpha}$, when the deuterated substrate is used.

For further quantitative analysis of the intermolecular noncompetitive kinetic deuterium isotope effects, we followed Northrop's abbreviations (*16*), where ^DV and $^D(V/K)$ are the kinetic deuterium isotope effects on V_{max} and V_{max}/K_m, respectively. According to this description, a relatively large intermolecular isotope effect was observed for V_{max}, whereas $^D(V/K)$ was masked for the catalytic reaction by $P450_{SP\alpha}$, as shown in Table 1.

Deuterium Effect on Enzymatic Reactions Catalyzed by $P450_{BS\beta}$. $P450_{BS\beta}$ also catalyzes the hydroxylation reaction of myristic acid with H_2O_2, as in the case for $P450_{SP\alpha}$, but the reaction products are both the α- and β-hydroxylated (−OH) myristic acids. Their proportions were 37% for α-OH and 63% for β-OH myristic acid. We used [2,2-d_2]- and d_{27}-myristic acids in place of the nondeuterated substrate to examine the deuteration effect on the enzymatic reaction and on the α-OH/β-OH product ratio (Table 1). In the reaction using [2,2-d_2]-myristic acid, both kinetic parameters, V_{max} and K_m, were hardly altered, compared with the corresponding values of the reaction using the nondeuterated substrate. Consequently, the total amount of the hydroxylated products was unaltered. However, the reaction products were 9% of the α-OH and 91% of the β-OH products. We also analyzed the kinetic parameters in the formation of α-OH and β-OH products separately. As presented in Table 2, it was found that the ^DV value was 6.1 for α-OH formation, while it was 0.7 for β-OH formation. Upon deuteration of the α-position of myristic acid, the α-OH formation rate was largely decreased, but the β-OH formation rate was increased to compensate for the decrease in the α-OH formation rate, resulting in no change in the ^DV value in the total hydroxylated product formation.

Upon deuteration of all the hydrogen atoms in myristic acid (d_{27}-myristic acid), the α-OH/β-OH product ratio was apparently unchanged from that with the nondeuterated substrate, i.e., 27% of the α-OH and 73% of the β-OH, but the V_{max} and K_m values were dramatically changed, as shown in Table 1. The ^DV values for α- and β-hydroxylation of d_{27}-myristic acid were 6.7 and 5.2, respectively (Table 2). The ^DV and $^D(V/K)$ values for $P450_{BS\beta}$ in the total product formation were basically the same as those for $P450_{SP\alpha}$ (Table 1), suggesting that the reaction mechanism is the same between $P450_{SP\alpha}$ and $P450_{BS\beta}$, although the site specificity is different.

Dissociation Constants of Substrates to $P450_{BS\beta}$. In the kinetic analyses stated above, it was notable that the K_m values were decreased in parallel with the decrement of the V_{max}, and the $^D(V/K)$ values were thus masked in both cases of the $P450_{SP\alpha}$ and $P450_{BS\beta}$ reactions. For comparison, we estimated dissociation constants (K_d) of nondeuterated and d_{27}-myristic acids for $P450_{BS\beta}$ by spectral analyses. Each substrate induced small but significant spectral changes for $P450_{BS\beta}$ of so-called "type I substrate difference spectra" (data not shown). The K_d value for d_{27}-myristic acid (14 ± 2.1 μM) was almost the same as that for nondeuterated

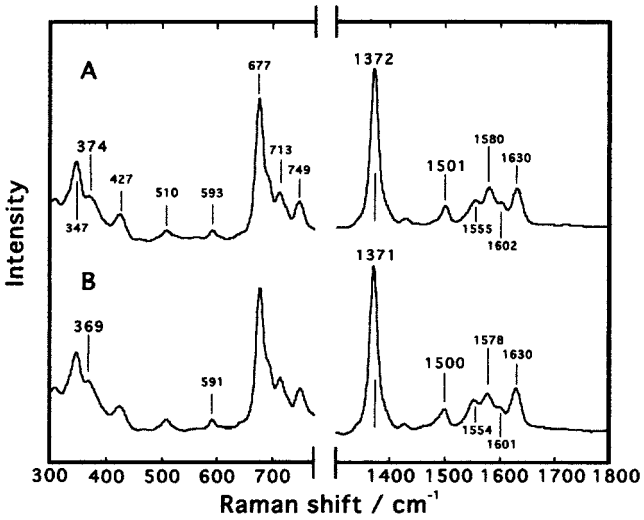

FIGURE 2: High (1300−1800 cm^{-1}) and low (300−800 cm^{-1}) frequency regions of the resonance Raman spectra of $P450_{BS\beta}$ in the ferric-resting state (A) in the absence and (B) presence of myristic acid (0.5 mM). The samples were dissolved in the buffer solution containing 100 mM HEPES (pH7.4) and 20% glycerol. The sample concentration was 50 μM. All spectra were obtained at 413 nm excitation with a laser power lower than 25 mW at the sample.

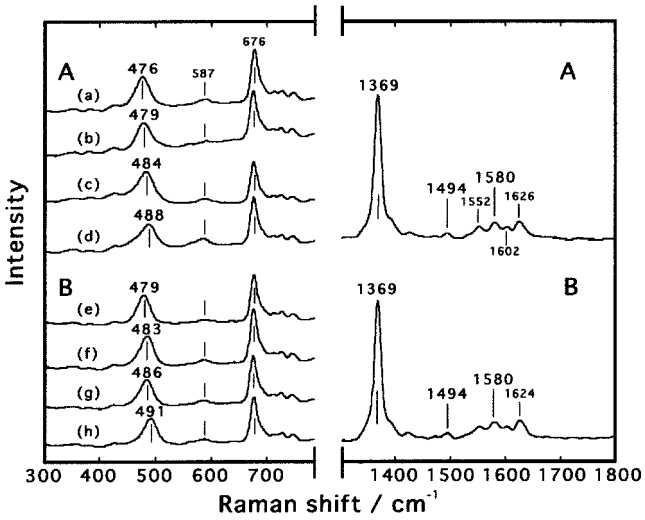

FIGURE 3: High (1300−1800 cm^{-1}) and low (300−800 cm^{-1}) frequency regions of the resonance Raman spectra of $P450_{BS\beta}$ in the ferrous−CO complex (A) in the absence and (B) presence of myristic acid (0.5 mM). In the left column, spectra of the isotopic CO complexes are shown: (a) $^{13}C^{18}O$, (b) $^{12}C^{18}O$, (c) $^{13}C^{16}O$, and (d) $^{12}C^{16}O$ in (A); and (e) $^{13}C^{18}O$, (f) $^{12}C^{18}O$, (g) $^{13}C^{16}O$, and (h) $^{12}C^{16}O$ in (B). The sample condition was the same as indicated in Figure 2. All spectra were obtained at 441 nm excitation with a laser power lower than 5 mW at the sample.

myristic acid (16 ± 2.4 μM). Since no significant change was induced in the optical spectrum of $P450_{SP\alpha}$ upon addition of any fatty acids (*17*), we could not obtain K_d values for the substrates to test the reaction mechanism of $P450_{SP\alpha}$.

Resonance Raman Spectra of $P450_{BS\beta}$. To characterize the heme environmental structure of peroxygenase P450s, we measured the resonance Raman spectra of $P450_{BS\beta}$ in the ferric and ferrous−CO forms in the presence or absence of myristic acid. We were unable to measure the Raman spectra of $P450_{SP\alpha}$, because the protein precipitated under irradiation of the laser.

(A) Ferric-Resting State. Figure 2 shows the resonance Raman spectra of $P450_{BS\beta}$ in the ferric-resting state. In the high-frequency region of the substrate-free form (right column in Figure 2A), the ν_4 and ν_3 bands were observed at 1372 and 1501 cm^{-1}, respectively. The positions of these bands indicated that the iron in the ferric-resting and the substrate-free form of $P450_{BS\beta}$ was a hexa-coordination in a low-spin state (*18*), as in the case for usual P450s (*19*). However, the ν_4 and ν_3 bands, as well as the others, did not change in their position upon addition of myristic acid to the enzyme solution (right column in Figure 2B). This observation was in sharp contrast to those for the substrate-bound forms of monooxygenase P450s (*19*), in which the ν_4 and ν_3 bands were usually observed at 1374 and 1488 cm^{-1}, respectively. While the heme iron in the usual P450s changed to a penta-coordination in a high-spin state upon substrate binding (*19*, *20*), the iron of $P450_{BS\beta}$ is still a hexa-coordination in a low-spin state even in the substrate-bound form. Corresponding to these observations in the high-frequency region, the spectra of $P450_{BS\beta}$ in the low-frequency region (left column in Figure 2) are basically indistinguishable between the substrate-free and -bound forms. The only difference was observed in the position of the band at 374 cm^{-1}, which can be assigned to the bending mode of the heme propionate, on the basis of the spectral comparison with myoglobin (*21*, *22*). The band was shifted from 374 to 369 cm^{-1} upon addition of myristic acid to the enzyme. The binding of myristic acid to $P450_{BS\beta}$ possibly influences conformations around the heme propionates.

(B) Ferrous−CO Complex of $P450_{BS\beta}$. Figure 3 shows the resonance Raman spectra of $P450_{BS\beta}$ in the ferrous−CO complex. The positions of the ν_4 (1369 cm^{-1}), ν_3 (1494 cm^{-1}), and ν_2 (1580 cm^{-1}) bands observed in the high-frequency region (right column in Figure 3A) were typical for the ferrous iron in a hexa-coordination and low-spin state. These bands were unaltered in their positions when myristic acid bound to $P450_{BS\beta}$ (right column in Figure 3B). On the other hand, the Fe−CO stretching frequency (νFe−CO) was observed at 488 cm^{-1} in the spectra of the low-frequency region [Figure 3A(d)]. When ^{13}CO, $C^{18}O$, or $^{13}C^{18}O$ was bound in place of CO, the νFe−CO band shifted to 484, 479, and 476 cm^{-1}, respectively, as shown in Figure 3A(c), (b), and (a). This shift pattern indicated the linear Fe−C−O unit. The νFe−CO band shifted by 3 cm^{-1} to the higher frequency region, and was observed at 491 cm^{-1} in the substrate-bound form [Figure 3B(h)]. This band shifted to 486, 483, and 479 cm^{-1} for the ^{13}CO, $C^{18}O$, and $^{13}C^{18}O$ complexes, respectively [Figure 3B(g), (f), and (e)]. The 3 cm^{-1} shift caused by myristic acid binding was small but significant, suggesting changes in the protein conformation or chemical environment around the iron-bound CO in $P450_{BS\beta}$.

DISCUSSION

Characteristics of Enzymatic Reactions by Peroxygenase P450s. In the present study, we found that the deuterium substitution for hydrogen atoms of the substrate (myristic acid) dramatically affected both the V_{max} and K_m in the enzymatic reactions of peroxygenases $P450_{SP\alpha}$ and $P450_{BS\beta}$. It was noteworthy to be found that ^{D}V was altered, but $^{D}(V/K)$ was masked in the reactions. The observations for $P450_{SP\alpha}$ and $P450_{BS\beta}$ were in sharp contrast to those for the

Scheme 1

$$E + S \underset{k_2}{\overset{k_1}{\rightleftharpoons}} ES \xrightarrow{k_3} E + P$$

usual monooxygenase P450s reported previously, in which the effects of the deuterium substitution of substrates were observed for both ^{D}V and $^{D}(V/K)$ (*10*). To our knowledge, one exception was reported by Ottoboni et al. (*23*) for the oxidation of 1-methyl-4-phenyl-1,2,3,6-tetrahydropyridine by P450 1A1, in which $^{D}(V/K)$ was masked.

In the classical and simple Michaelis−Menten model of enzymatic reactions (Scheme 1), the K_m value can be considered to be an expression of the dissociation constant (K_d) for a substrate when the substrate dissociation rate (k_2) is much larger than the product formation rate (k_3). On the other hand, we can express the deuteration effect on the reaction, $^{D}(V/K)$, as follows: $^{D}(V/K) = (^{D}V + k_3/k_2)/(1 + k_3/k_2)$. Under the condition $k_2 \gg k_3$, the $^{D}(V/K)$ value must be nearly equal to the ^{D}V value. Namely, upon deuteration of the substrate, the V_{max} is affected, but the *K*m is not. This has been the case for the usual monooxygenase P450s reported so far.

In contrast, the present results on peroxygenases $P450_{SP\alpha}$ and $P450_{BS\beta}$, in which $^{D}(V/K)$ is almost masked, imply that k_3 would be larger than k_2 ($k_2 \ll k_3$). Under this kinetic feature, the K_d value for a substrate must be different from the K_m value. Indeed, the K_d value of $P450_{BS\beta}$ for myristic acid (14 μM), which was spectrophotometrically determined, is not identical to the K_m value (58 μM). As a consequence of the deuteration effect, the k_3 step in the reaction of $P450_{BS\beta}$ with the d_{27}-substrate was smaller than the other rate constants, giving a K_m value (17 μM) apparently close to the K_d value. It was, therefore, concluded for the fatty acid-hydroxylating reactions with H_2O_2 catalyzed by $P450_{SP\alpha}$ and $P450_{BS\beta}$ that the product formation rate (k_3) is relatively fast, compared with the substrate dissociation rate (k_2) from the enzyme. The relatively large k_3 could be one of the driving forces for the high turnover of the H_2O_2-dependent hydroxylation by peroxygenases $P450_{SP\alpha}$ and $P450_{BS\beta}$.

Substrate Recognition and Site Specificity of the Reaction. Monooxygenase P450s such as P450BM3 catalyze the hydroxylation of long-chain fatty acids as in the case for $P450_{SP\alpha}$ and $P450_{BS\beta}$. However, the site specificities of the reactions are entirely different from each other; P450BM3 hydroxylates the ω-1 and ω-2 positions of the fatty acid, while $P450_{SP\alpha}$ and $P450_{BS\beta}$ give the α- or β-OH products. The difference in the reaction site is suggestive of differences in the substrate recognition by the enzymes. The substrate recognition in P450BM3 has been well-defined on the basis of its crystal structure (*24*): the carboxylate of the fatty acid electrostatically interacts with the Arg47 guanidyl group present on the protein surface, and the alkyl chain entering into the active site is stabilized through some hydrophobic contacts with the Leu, Val, and Ala residues present in the channel. As a result, the ω-1 and ω-2 positions of the fatty acid are located closest to the active site, producing the (ω-1)- and (ω-2)-OH products in the catalytic reaction.

In contrast, the carboxylate of the fatty acid should be located in close proximity to the heme iron in the active site of peroxygenases $P450_{SP\alpha}$ and $P450_{BS\beta}$, because the α- or β-position of the substrate reacts. In the Raman measurements of the present study, we found that a water molecule

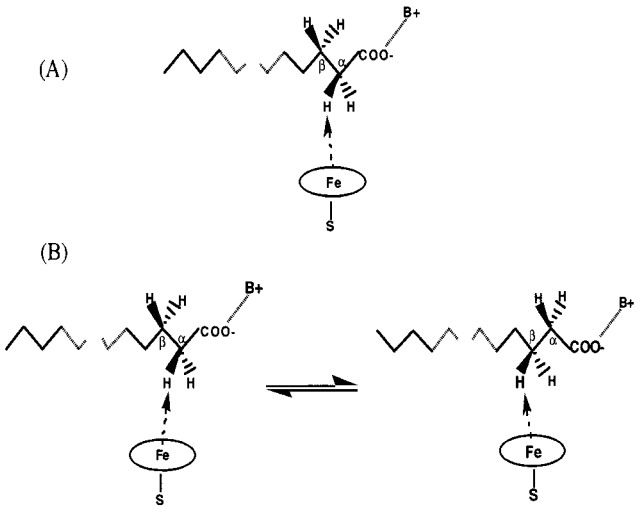

FIGURE 4: Possible configuration of the substrate relative to the heme moiety of peroxygenases $P450_{SP\alpha}$ (A) and $P450_{BS\beta}$ (B). B^+ indicates a basic amino acid residue.

was present at the sixth coordination site of the heme ferric iron in $P450_{BS\beta}$, irrespective of the presence or absence of the substrate. In the Raman spectra of the ferrous−CO complex of $P450_{BS\beta}$, the νFe−CO stretching band (488 cm^{-1}) was located in a higher frequency region than that of P450BM3 (471 cm^{-1}) (*19*), the heme pocket of which is hydrophobic. All these spectral data are suggestive of a polar environment of the sixth iron coordination site in $P450_{BS\beta}$. The polar environment would allow the location of the polar carboxylate of the fatty acid substrate. Interestingly, we recently obtained evidence that Arg242 of the distal helix of $P450_{BS\beta}$ interacts with the substrate and, thus, such a basic residue stabilizes substrate binding (*15*).

As evidenced by the isotope effect on the νFe−CO stretching band in the Raman spectra of $P450_{BS\beta}$, CO linearly binds to the ferrous iron. However, the linear Fe−C−O geometry is slightly bent upon substrate binding, because the νFe−CO stretching band moved from 488 to 491 cm^{-1}. The bent configuration was possibly caused by the steric hindrance exposed by the bound substrate. Therefore, the ligand-binding pocket of $P450_{BS\beta}$ is polar, and the substrate can bind to the enzyme very closely to the sixth ligand.

In $P450_{SP\alpha}$, the α-position of the fatty acid should be closest to the heme iron (Figure 4A), resulting in only α-hydroxylation. On the other hand, as determined from the ratio of the α-OH/β-OH products, the α- and β-positions would be almost equally close to the heme iron in $P450_{BS\beta}$. In the present study, it is of note that the deutration of only the α-position of the substrate ([2,2-d_2]-myristic acid) largely decreased the V_{max} value for α-hydroxylation, while it increased the V_{max} value for β-hydroxylation (Table 2), resulting in no change in the V_{max} for total product formation, but a large change in the α-OH/β-OH product ratio. These findings may be explained by the kinetic model of a branched pathway (*25*) (see Scheme 2), where two distinct products (P_α, P_β) are formed from one substrate (S) and two activated substrate−enzyme tertiary complexes (ES_α and ES_β) are in equilibrium: P_α is produced from ES_α, and P_β from ES_β. For example, S_α and S_β may be rotational isomers of the bound substrate (see Figure 4B), and P_α is the α-OH product and P_β is the β-OH product. When the P_α formation is

Scheme 2

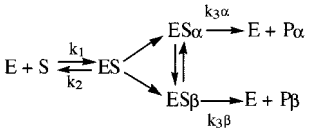

Scheme 3

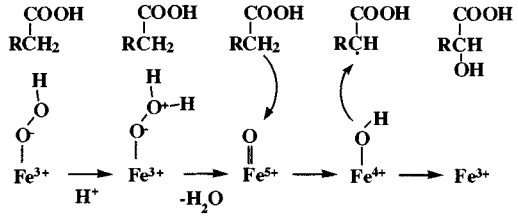

reduced by deuteration of α-H, ES_β will increase, resulting in an increment in the P_β formation.

Possible Mechanism of Hydroxylation Reaction by Peroxygenase P450. In the usual P450 monooxygenation reactions, O_2, two electrons, and two protons are essential requirements, and proton transfer from solvent water to the heme moiety, which is coupled with the second electron transfer, is a rate-determining step (*8*). In contrast, peroxygenases $P450_{SP\alpha}$ and $P450_{BS\beta}$ utilize H_2O_2 as an oxidant in the hydroxylation reaction of fatty acids in place of O_2, two electrons, and two protons. This implies that proton transfer is not involved in the peroxygenase reaction, i.e., the self-sufficient reaction. When D_2O was used as a reaction solvent, in place of H_2O, the peroxygenase reaction was unaffected (data not shown). In addition, it should be noted that the highly conserved Thr residue, which is found in usual monooxygenase P450s, is probably replaced with another residue (Pro or Ala) in both $P450_{SP\alpha}$ and $P450_{BS\beta}$, as was revealed from the primary sequence alignment (*3*, *4*), suggesting an absence of the proton delivery pathway from solvent water to the heme active site.

Concerning the hydroxylation reaction catalyzed by monooxygenase P450s, the hydrogen abstraction−oxygen rebound mechanism shown in Scheme 3 has been generally accepted. In this mechanism, the hydroperoxo−iron species is first converted to an iron−oxo species [either $Fe^{5+}O$ or $Fe^{4+}O$ (porphyrin π-cation radical)], and the resultant iron−oxo species abstracts a hydrogen atom from the substrate to produce an iron−hydroxy species and an alkyl radical intermediate. The alkyl radical then displaces the hydroxyl from the iron in a process termed "oxygen rebound".

This mechanism is apparently applicable for the α- and β-hydroxylation by $P450_{SP\alpha}$ and $P450_{BS\beta}$. It seems reasonable to consider that the α-H or β-H, which are located in close proximity to the heme site, are abstracted by the putative iron−oxo species, and that this step is a rate-determining step of the catalytic reaction. This consideration is apparently consistent with a previous report from another study on P450 reactions (*13*), in which a deuterium intermolecular noncompetitive isotope effect was interpreted as indicating that hydrogen atom abstraction is a rate-limiting step. However, the peroxide O−O bond cleavage (the first step of Scheme 3) must usually be supported by some functional residues. For example, His and Arg act as acid−base catalysts for the peroxide O−O bond cleavage by peroxidases. As stated above, the functional Thr residue seems to be absent in the

Scheme 4

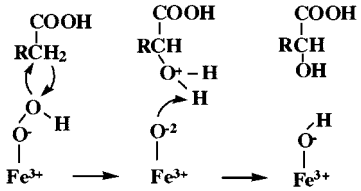

active site of $P450_{SP\alpha}$ and $P450_{BS\beta}$. This is apparently supported by our recent finding that these ferric enzymes could not react with H_2O_2 in the absence of the substrate; that is, their optical absorption spectra were hardly changed by the addition of H_2O_2 (data not shown). The catalytic reaction turns over, of course, in the presence of the substrate. Therefore, we suggest that the active sites of $P450_{SP\alpha}$ and $P450_{BS\beta}$ themselves do not have a system to support the peroxide O−O bond cleavage, and that substrate binding is essential for the catalytic reaction of these peroxygenases. If substrate binding changes protein conformations suitable for the peroxide O−O bond cleavage, the reaction mechanism in Scheme 3 would be acceptable for $P450_{SP\alpha}$ and $P450_{BS\beta}$.

Recently, Newcomb, Hollenberg, Coon, and co-workers (*9*) proposed the so-called "cationic rearrangement mechanism," as shown in Scheme 4, in which the OH^+ element (electrophile) from the hydroperoxide−iron species is inserted into the substrate. This mechanism may be considerable given the hydroxylation by $P450_{SP\alpha}$ and $P450_{BS\beta}$, because, in this mechanism, the substrate can support peroxide O−O bond cleavage and functional residues such as conserved Thr are not necessarily required. However, here we should consider the proposed mechanism of P450eryF (*26*), one of a few monooxygenase P450s of which the functional Thr residue is substituted with another hydrophobic residue such as Ala. In this mechanism, the 5-hydroxyl group of the substrate, 6-deoxyerythrolide B, let the water molecule position to operate as an acid catalyst required for cleaving dioxygen. Namely, the hydroxyl group apparently acts instead of the functional Thr residue, and the O−O band would be cleaved by the water to produce an iron−oxo species. This mechanism is very attractive, because the carboxylate of $P450_{SP\alpha}$ and $P450_{BS\beta}$ substrates would be positioned nearby the heme iron and, thus, an oxygen of the carboxylate may act in the same manner as the P450eryF mechanism. In any event, details should be discussed following the determination of the structures of $P450_{SP\alpha}$ or $P450_{BS\beta}$ in the substrate-free and -bound forms.

REFERENCES

1. Nelson, D. R., Kamataki, T., Waxman, D. J., Guengerich, F. P., Estabrook, R. W., Feyereisen, R., Gonzalez, F. J., Coon, M. J., Gunsalus, I. C., Gotoh, O., Okuda, K., and Nebert, D. W. (1993) *DNA Cell Biol. 12*, 1−51.
2. Matsunaga, I., Sumimoto, T., Ueda, A., Kusunose, E., and Ichihara, K. (2000) *Lipids 35*, 365−371.
3. Matsunaga, I., Ueda, A., Fujiwara, N., Sumimoto, T., and Ichihara, K. (1999) *Lipids 34*, 841−846.
4. Matsunaga, I., Yokotani, N., Gotoh, O., Kusunose, E., Yamada, M., and Ichihara, K. (1997) *J. Biol. Chem. 272*, 23592−23596.
5. Matsunaga, I., Yamada, M., Kusunose, E., Miki, T., and Ichihara, K. (1998) *J. Biochem. (Tokyo) 124*, 105−110.
6. Matsunaga, I., Yamada, M., Kusunose, E., Nishiuchi, Y., Yano, I., and Ichihara, K. (1996) *FEBS Lett. 386*, 252−254.

7. Matsunaga, I., Kusunose, E., Yano, I., and Ichihara, K. (1994) *Biochem. Biophys. Res. Commun. 201*, 1554−1560.
8. Sono, M., Roach, M. P., Coulter, E. D., and Dawson, J. H. (1996) *Chem. Rev. 96*, 2841−2867.
9. Newcomb, M., Shen, R., Choi, S.-Y., Toy, P. H., Hollenberg, P. F., Vaz, A. D. N., and Coon, M. J. (2000) *J. Am. Chem. Soc. 122*, 2677−2686.
10. Guengerich, F. P., Peterson, L. A., and Bocker, R. H. (1988) *J. Biol. Chem. 263*, 8176−8183.
11. Rettie, A. E., Boberg, M., Rettenmeier, A. W., and Baillie, T. A. (1988) *J. Biol. Chem. 263*, 13733−13738.
12. Rettie, A. E., Sheffels, P. R., Korzekwa, K. R., Gonzalez, F. J., Philpot, R. M., and Baillie, T. A. (1995) *Biochemistry 34*, 7889−7895.
13. Guan, X., Fisher, M. B., Lang, D. H., Zheng, Y. M., Koop, D. R., and Rettie, A. E. (1998) *Chem.-Biol. Interact. 110*, 103−121.
14. Matsunaga, I., Sumimoto, T., Kusunose, E., and Ichihara, K. (1998) *Lipids 33*, 1213−1216.
15. Matsunaga, I., Ueda, A., Sumimoto, T., Ichihara, K., Ayata, M., and Ogura, H. (2001) *Arch. Biochem. Biophys. 394*, 45−53.
16. Northrop, D. B. (1975) *Biochemistry 14*, 2644−2651.
17. Imai, Y., Matsunaga, I., Kusunose, E., and Ichihara, K. (2000) *J. Biochem. (Tokyo) 128*, 189−194.
18. Spiro, T. G., Ed. (1988) *Biological Application of Raman Spectroscopy*, Vol. 3, John Wiley & Sons, New York.
19. Deng, T.-G., Proniewicz, L. M., Kincaid, J. R., Yeom, H., Macdonald, I. D. G., and Sliger, S. G. (1999) *Biochemistry 38*, 13699−13706.
20. Champion, P. M., Gunsalus, I. C., and Wagner, G. C. (1978) *J. Am. Chem. Soc. 100*, 3743−3751.
21. Feis, A., Marzocchi, M. P., Paoli, M., and Smulevich, G. (1994) *Biochemistry 33*, 4577−4583.
22. Hu, S., Morris, I. K., Singh, J. P., Smith, K. M., and Spiro, T. G. (1993) *J. Am. Chem. Soc 115*, 12446−12458.
23. Ottoboni, S., Carlson, T. J., Trager, W. F., Castagnoli, K., and Castagnoli, N., Jr. (1990) *Chem. Res. Toxicol. 3*, 423−427.
24. Li, H., and Poulos, T. L. (1997) *Nat. Struct. Biol. 4*, 140−146.
25. Higgins, L., Bennett, G. A., Shimoji, M., and Jones, J. P. (1998) *Biochemistry 37*, 7039−7046.
26. Cupp-Vickery, J. R., Han, O., Hutchinson, C. R., and Poulos, T. L. (1996) *Nat. Struct. Biol. 3*, 632−637.

BI011883P